Review Article
Fiber tracking: principles and strategies – a technical review

Susumu Mori* and Peter C. M. van Zijl

Johns Hopkins University School of Medicine, Department of Radiology and Radiological Science and Kennedy Krieger Institute, F.M. Kirby Research Center for Functional Brain Imaging, Baltimore, MD 21205, USA

ABSTRACT: The state of the art of reconstruction of the axonal tracts in the central nervous system (CNS) using diffusion tensor imaging (DTI) is reviewed. This relatively new technique has generated much enthusiasm and high expectations because it presently is the only approach available to non-invasively study the three-dimensional architecture of white matter tracts. While there is no doubt that DTI fiber tracking is providing exciting new opportunities to study CNS anatomy, it is very important to understand its limitations. In this review we therefore assess the basic principles and the assumptions that need to be made for each step of the study, including both data acquisition and the elaborate fiber reconstruction algorithms. Special attention is paid to situations where complications may arise, and possible solutions are reviewed. Validation issues and potential future directions and improvements are also discussed. Copyright © 2002 John Wiley & Sons, Ltd.

KEYWORDS: axonal tracking; diffusion tensor imaging, DTI; brain; methods

INTRODUCTION

Experimental evidence has shown that water diffusion is anisotropic in organized tissues such as muscles[1,2] or brain white matter.[3] In the last decade, the quantitative description of this anisotropy with diffusion tensor imaging (DTI) has become well established in the research environment and its first applications in the clinic are now being reported. These applications employ both the directional anisotropy that can be measured by DTI[4,5] as well as removal of this anisotropy through the use of the tensor trace.[6–8] For example, DTI is presently being explored as a research tool to study brain development,[9,10] multiple sclerosis,[11,12] amyotrophic lateral sclerosis (ALS),[13] stroke,[14,15,] schizophrenia[16,17] and reading disability,[18] while trace imaging has become an essential part of clinical acute stroke assessment.[19–22] As first shown by Basser *et al*,[4] the diffusion ellipsoid obtained from DTI can not only provide a quantitative

orientation-independent measure of diffusion anisotropy,[23,24] but also the predominant direction of water diffusion in image voxels.[25–27] However, it was not until the end of the decade and the beginning of the new millenium that the first successful *in vivo* fiber tracking results were published.[28–42] The reason for this time lag between the availability of the tensor diagonalization techniques that provide the vector information and the actual mapping of the fibers is due to the inherent complexity of connecting these macroscopic voxel-based vectors in a reproducible three-dimensional manner. At present, new tracking algorithms are being developed rapidly, and in this review we will provide an overview of the current state-of-the-art approaches. In order to better utilize this promising technology, it is important to understand the basis of the anisotropy contrast in DTI and the limitations imposed by using a macroscopic technique to visualize microscopic restrictions. These basics are briefly reviewed, while a more comprehensive overview is presented by Beaulieu *et al*.[43] Recent technologies that have been demonstrated to allow the visualization of three-dimensional (3D) fiber tracts are reviewed and discussed with respect to their potential and limitations regarding the determination of propagation, termination, branching and editing of tracts. Limitations and several techniques that may minimize them are described. Recent work related to the validation of using DTI-based fiber tracts to describe white matter connections is also discussed.

Correspondence to: S. Mori, Johns Hopkins University School of Medicine, Department of Radiology, 217 Traylor Building, 720 Rutland Ave, Baltimore, MD 21205, USA.
Email: susumu@mri.jhu.edu
Abbreviations used: ALS, amyotrophic lateral sclerosis; CNS, central nervous system; CST, cortio-spinal tract; DTI, diffusion tensor imaging; FACT, fiber assignment by continuous tracking; FPT, frontopontine tract; ROI, region of interest; SLF, superior longitudinal fasciculus; SNR, signal-to-noise ratio; TPOPT, temporo parietalo occipital pontine tract.
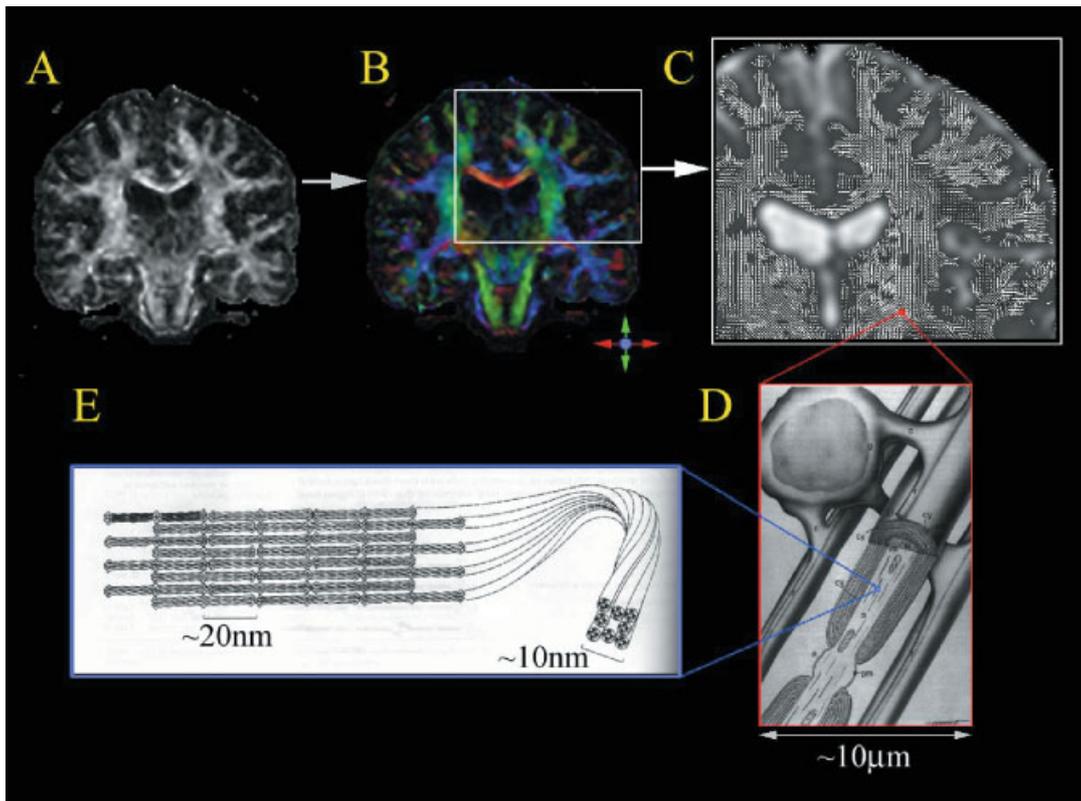
Figure 1. Schematic diagram of the white matter structure and its relationship with the information provided by DTI-based images, such as anisotropy maps (A), have sufficient resolution to segment white and gray matter. By incorporating DTI orientation information, white matter can be parcellated into various tracts using a color-coded map (B) or a vector map (C). The image resolution is sufficient to delineate large white matter tracts, which mostly consist of neuroglia and axons that are largely running parallel. A pixel thus contains bundles of axons and neuroglial cells (D). Note that the size of a pixel (C) is on the order of mm but that the size of the cells (D) is on the order of μm. The axon is filled with neuronal filaments (E) running along its longitudinal axis, which may contribute in superimposing anisotropy on the direction of water diffusion. In the color-coded map, red indicates fibers running along the right–left direction, green inferior–superior, and blue anterior–posterior (perpendicular to the plane). The figures (D) and (E) were reproduced from Carpenter[49] and Alberts et al.[64] respectively with permission

CELLULAR ARCHITECTURE SUPERIMPOSES ORIENTATION ON THE RANDOM MOTION OF WATER MOLECULES

DTI essentially provides two types of information about the property of water diffusion; the extent of diffusion anisotropy and its orientation. By assuming that the largest principal axis of the diffusion tensor aligns with the predominant fiber orientation in an MRI voxel, we can obtain 2D or 3D vector fields that represent the fiber orientation at each voxel. The 3D reconstruction of tract trajectories, or tractography, is a natural extension of such vector fields. Before further describing tractography, it is important to discuss what exactly DTI measures and how the data relate to the tract trajectories we are trying to derive from the measurement.

In typical DTI measurements, the voxel dimensions are on the order of 1–5 mm and DTI measures the averaged diffusion properties of water molecules inside it. This voxel size is usually small enough to distinguish white and gray matter [Fig. 1(A)]. The white matter consists of tracts that are running along various directions and are large enough to discern visually [Fig. 1(B) and (C)]. Very often, image resolution is sufficiently high for the white matter tracts to contain several voxels. The white matter tracts, in turn, consist of densely packed axons (neuronal projections) in addition to various types of neuroglia and other small populations of cells [Fig. 1(D)]. Inside the voxel, water molecules are distributed between these cell types and the extracellular space (80–85% are intracellular). Thus, even a voxel within a single white matter tract consists of very inhomogeneous environment, and water molecules are likely to experience high anisotropy as judged from the cytoarchitecture of the axon [Fig. 1(D) and (E)]. Inside an axon, water molecules are surrounded by high concentration of neuronal filaments, which are

polymers of protein molecules. Each monomer protein has a molecular weight of 50–150 kDa. The neuronal filament is far larger than that, and multiple filament bundles are densely packed in the axon. The axonal membrane as well as the well-aligned protein fibers within an axon restrict water diffusion perpendicular to the fiber orientation, leading to anisotropic diffusion. Myelin sheaths that surround the axons may also contribute to the anisotropy for both intra- and extra-cellular water. These contributions have been studied in detail by Beaulieu[43] using non-myelinated axons, showing that the contribution of myelin may be significant, but that the axonal contribution dominates. In addition to the inhomogeneity in terms of the cellular environment of water molecules, inhomogeneity of axonal orientation within one voxel is also an important factor to be considered. Despite this multi-directional environment, previous DTI studies have shown that water diffusion in many regions of the white matter is highly anisotropic [see Fig. 1(A)] and that the orientation of the largest principal axis aligns to the predominant axonal orientation.[3,44–47] However, when studying axonal architecture using DTI, it is very important to understand the limitations arising from the inhomogeneity of the water environment. First, the conventional DTI data acquisition and processing methods may not be able to properly handle a voxel containing more than one population of axonal tracts with different orientations. This issue will be discussed in more detail below. Second, DTI cannot provide information on cellular-level axonal connectivity. Multiple axons from individual cells may merge into or branch out from one voxel. Within a voxel, cellular-level axonal information of multiple compartments is averaged. The third important limitation is that afferent and efferent pathways of axonal tracts cannot be judged from the direction of water diffusion.

Without resorting to DTI, there is a fair amount of anatomical knowledge on the human white matter structure based on classical anatomical studies (see for example,[47–50]) and the question that often arises is what tractography will be able to provide in addition to this. Based on the relative size of the voxel and the human brain, it should be safe to say that it can reveal macroscopic 3D architectures of the white matter and constituent white matter tracts [Fig. 1(A)–(B)]. Thus, DTI and tractography provide us with a new opportunity to investigate such structures in living humans and to assess changes due to brain disease. Bearing the basic limitations in mind, we will now discuss recent 3D tract reconstruction techniques that employ 3D vector fields obtained from DTI measurements.

FIBER RECONSTRUCTION TECHNIQUES

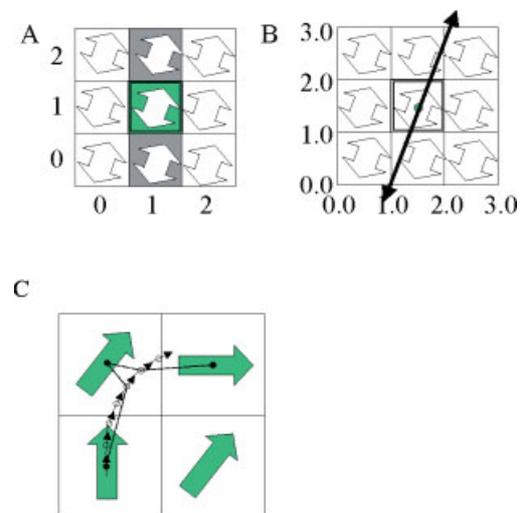Assuming that the orientation of the largest component of the diagonalized diffusion tensor represents the orienta-

Figure 2. Schematic diagram of the linear line-propagation approach. Double-headed arrows indicate fiber orientations at each pixel. Tracking is initiated from the center pixel. In the discrete number field (A), the coordinate of the seed pixel is {1, 1}. If it is judged that the vector is pointing to {1, 2} and {1, 0}, shaded pixels are connected. In the continuous number field (B), the seed point is {1.50, 1.50} and a line, instead of a series of pixels, is propagated. (C) shows an example of the interpolation approach to perform nonlinear line propagation. Large arrows indicate the vector of the largest principal axis. For every step size, a distance-weighted average of nearby vectors is calculated. In this example, the vector orientations of two nearest pixels are averaged as the line is propagated

tion of dominant axonal tracts, DTI can provide a 3D vector field, in which each vector presents the fiber orientation. Currently, there are several different approaches to reconstruct white matter tracts, which can be roughly divided into two types. Techniques classified in the first category are based on line propagation algorithms that use local tensor information for each step of the propagation. The main differences among techniques in this class stem from the way information from neighboring pixels is incorporated to define smooth trajectories or to minimize noise contributions. The second type of approach is based on global energy minimization to find the energetically most favorable path between two predetermined pixels.

Line propagation techniques

Propagation approaches. The most intuitive way to reconstruct a 3D trajectory from a 3D vector field is to propagate a line from a seed point by following the local vector orientation. However, if a line is propagated simply by connecting pixels, which are discrete entities, the vector information contained at each pixel may not be fully reflected in the propagation. In the simple example illustrated in Fig. 2(A), axonal tracts are running along 30° from the vertical line. When applying the discrete

'pixel connection' approach, a judgment has to be made about which pixel should be connected (for instance, is the 30° vector angle pointing at pixel {1, 2} or {2, 2}?). No matter what the judgment is, it should be clear that this simple pixel connection scheme cannot represent the real tract even in such a simple case. The simplest way to convert the discrete voxel information into a continuous tracking line is to linearly propagate 'a line', in a continuous number field. This conversion from the discrete to continuous number field is shown in Fig. 2(B). In this example, the seed point is {1.50, 1.50} and a line propagates from this point following the vector orientation of the pixel with discrete coordinate {1, 1}. This line exits the pixel (discrete coordinate {1, 1}) to the next pixel (discrete coordinate {1, 2}) at the location {1.79, 2.00} in the continuous coordinate. By repeating this process, it is easy to see that the line can follow the actual tract (or pixels can be connected) more precisely. This linear propagation approach, which was dubbed FACT (fiber assignment by continuous tracking), was used for the first successful tract reconstruction, which was accomplished for a fixed rat brain and showed good agreement with histological knowledge.[28,30,31]

The simple linear approach demonstrated in Fig. 2(A, B) can be modified to create a smooth (curved) path, which should be more accurate when the curvature of a reconstructed line is steep with respect to imaging resolution. A schematic diagram of a simple interpolation approach that can achieve such a smooth path is shown in Fig. 2(C). In this example, the line is propagated with a small, predefined step size. Whenever it moves to a new coordinate, a distance-averaged vector orientation is calculated. In this most simple example, the average between two pixels closest to the new coordinate was used to draw a smooth line between pixels. In more rigorous approaches, diffusion tensors, rather than the vector of the largest principle axis, are interpolated at each coordinate as a line is being propagated.[32,35]

The choice between using the simple continuous approach or an interpolation technique depends on the degree of curvature of the tract of interest with respect to the imaging resolution. If resolution is low and kinks in the reconstructed path are evident, interpolation techniques should provide an advantage in accuracy. On the other hand, if the resolution is sufficiently high, the non-interpolating techniques offer faster calculation. For example, when using DTI images with $1 \times 1 \times 3$ mm resolution, the stretch of the corticospinal tract between the pons and the motor cortex has a rather small average angle of $7.8 \pm 5.8°$ (SD) between connecting pixels,[42] for which the effect of interpolation should be minimal. Recently, several interpolation techniques were compared using simulated data,[51] which will be discussed in the next section.

Termination criteria. Line propagation must be terminated at some point. The most intuitive termination criterion is the extent of anisotropy. In a low anisotropy region, such as gray matter, there may not be a coherent tract orientation within a pixel and the orientation of the largest principal axis is more sensitive to noise errors (for isotropic diffusion, the anisotropy information is dominated by noise and becomes purely random). The fractional anisotropy of the gray matter is typically in the range 0.1–0.2. Therefore, one simple termination approach is to set the threshold for tracking termination at 0.2. Another important criterion is the angle change between pixels. For the linear line propagation model, large errors occur if the angle transition is large. Even for the interpolation approach, it should be noted that the diffusion tensor calculation assumes that there is no consistent curvature of axonal tracts within a voxel. The presence of curvature violates the assumption that the diffusion process along any arbitrary axis is Gaussian, thereby invalidating the routine tensor calculation. Therefore, it is preferable to set a threshold that prohibits a sharp turn during line propagation. The significance of this angle-transition threshold depends on the particular trajectories of tracts of interest and the image resolution. An image resolution of 1–3 mm, for example, is high enough to smoothly reconstruct the curvature of trajectories of major tracts in the brainstem[42] and the cortico-cortical association fibers connecting the functional regions of the brain.[52] Under such favorable conditions, the angles between connected vectors are small and the termination criteria are dominated by the magnitude of the fractional anisotropy. However, for smaller tracts in environments that are structurally highly convoluted, such as sub-cortical U-fibers, the same resolution may be too coarse to smoothly represent the trajectories and, thus, analysis for the errors in tensor calculations and fiber tracking due to the curvature becomes more important. While at this moment there are no comprehensive simulation studies in this regard, some preliminary data on the effect of the turning radius on the tracking results in particular examples can be found in recent reports.[51,53]

Effect of noise on the accuracy of the tracking. The 3D vector field obtained from DTI contains noise and, as a consequence, the calculated vector direction may deviate from the real fiber orientation. One of the drawbacks of line propagation methods is that noise errors accumulate as the propagation becomes longer. The extent of these errors as a function of signal-to-noise ratio (SNR) has been evaluated for linear and interpolated models.[35,51,53] The results show a dependence on the shape of the trajectory, anisotropy, resolution and the particular interpolation method used. For example, in a helical trajectory model, the mean errors after 10 mm of tracking using non-interpolation and linear interpolation method were 0.19 vs 0.002 mm for infinite SNR and 0.55 vs 0.40 for a SNR of 30.[51] The noise effect can be reduced using smoothing or interpolation techniques, which averages vector or tensor information among
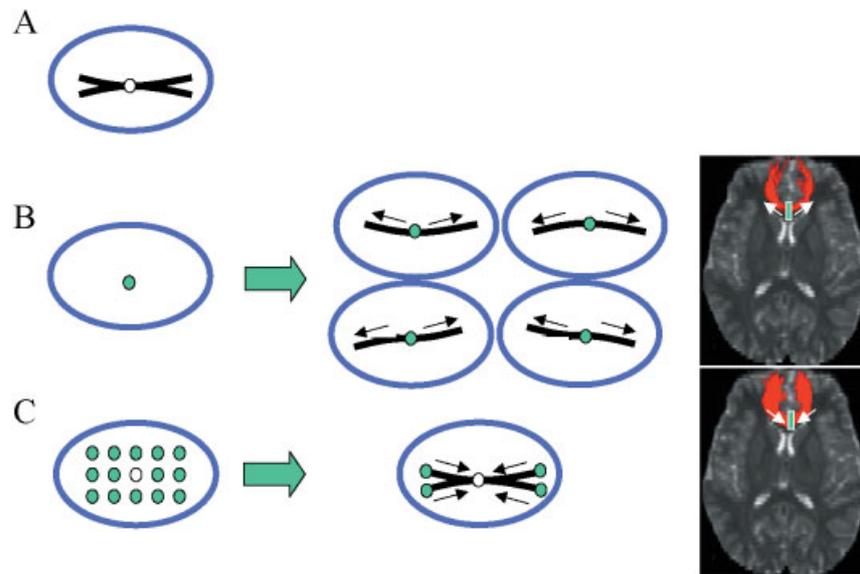
Figure 3. Schematic diagram of the difference between the single tracking (B) and exhaustive search approaches (C). Suppose (A) represents the shape of a white matter tract of interest with an anatomical landmark indicated by a white circle. If a tracking is initiated from the landmark, there are four possibilities for the results, each representing one branch of the tract (B). This is because a propagation result from one pixel can delineate only one line. Conversely, the line propagation can be initiated from all pixels and all propagation results that penetrate the anatomical landmark are searched, which leads to more comprehensive delineation of the tract of interest. The right column comparison the tracking results for these two approaches for the genu of the corpus callosum

neighboring pixels with a cost in the reduction in effective resolution. Several approaches to minimize the noise effects have also been suggested, such as approximation of a tensor field based on B-spline fitting[35] or 'regularization' of the tensor field based on a 'low curvature hypothesis'.[34] A detailed description of the latter approach has been given by Mangin *et al.*[54] While the tracking errors mentioned above might sound small, there is always a possibility that the errors in the line propagation by several pixels results in picking up adjacent and unrelated white matter tracts. Thus, tractography results should always be interpreted with caution. Limitations and errors of the tracking techniques and possible solutions will be further discussed below.

Branching. White matter tracts often have extensive branching, which renders tracking computationally complex. For example, bifurcation of a line during propagation is already a mathematically involved issue. From a programming point of view, this problem can be much more easily handled by merging two lines rather than splitting a line into two, for instance by using the brute force approach shown in Fig. 3.[32,42] In this approach, tracking is initiated from all pixels within the brain and tracking results that penetrate the pixel of interest are kept. In other words, instead of using the pixel of interest as a seed pixel, all pixels in the brain are used as seed pixels. When using the linear propagation model for a

data size of $256 \times 256 \times 60$, this exhaustive search takes about 15–30 min on a 900 MHz Pentium III processor.

Tract editing and white matter parcellation based on tractography. Results of the line propagation techniques depend heavily on the initial placement of reference pixels of interest. Suppose one is interested in the optic radiation, there are many choices to place a reference pixel of interest (POI) or a group of pixels (a region of interest, ROI). For instance, one can use the white matter close to the lateral geniculate nucleus (LGN), close to the visual cortex (VC), or anywhere in between the two areas. A powerful technique that can effectively search all seed pixels potentially containing the tracts of interest is the so-called multiple-ROI or tracking-editing technique.[32,42,52,55] In this approach, relatively large reference ROIs are drawn that contain the white matter close to the target gray matter. Examples are shown in Fig. 4, in which the anterior and posterior thalamic radiations are identified by using a two-ROI approach.[53] For example, the posterior thalamic radiation that contains the optic radiation was defined by one ROI at the pulvinor and another at the occipital lobe. Then, an exhaustive search, such as described above, was performed to identify all tracts that penetrate both ROIs. In this way, the reconstruction results for specific white matter tracts become less dependent on the locations of the initial POI or ROI. This technique is knowledge-based and existing
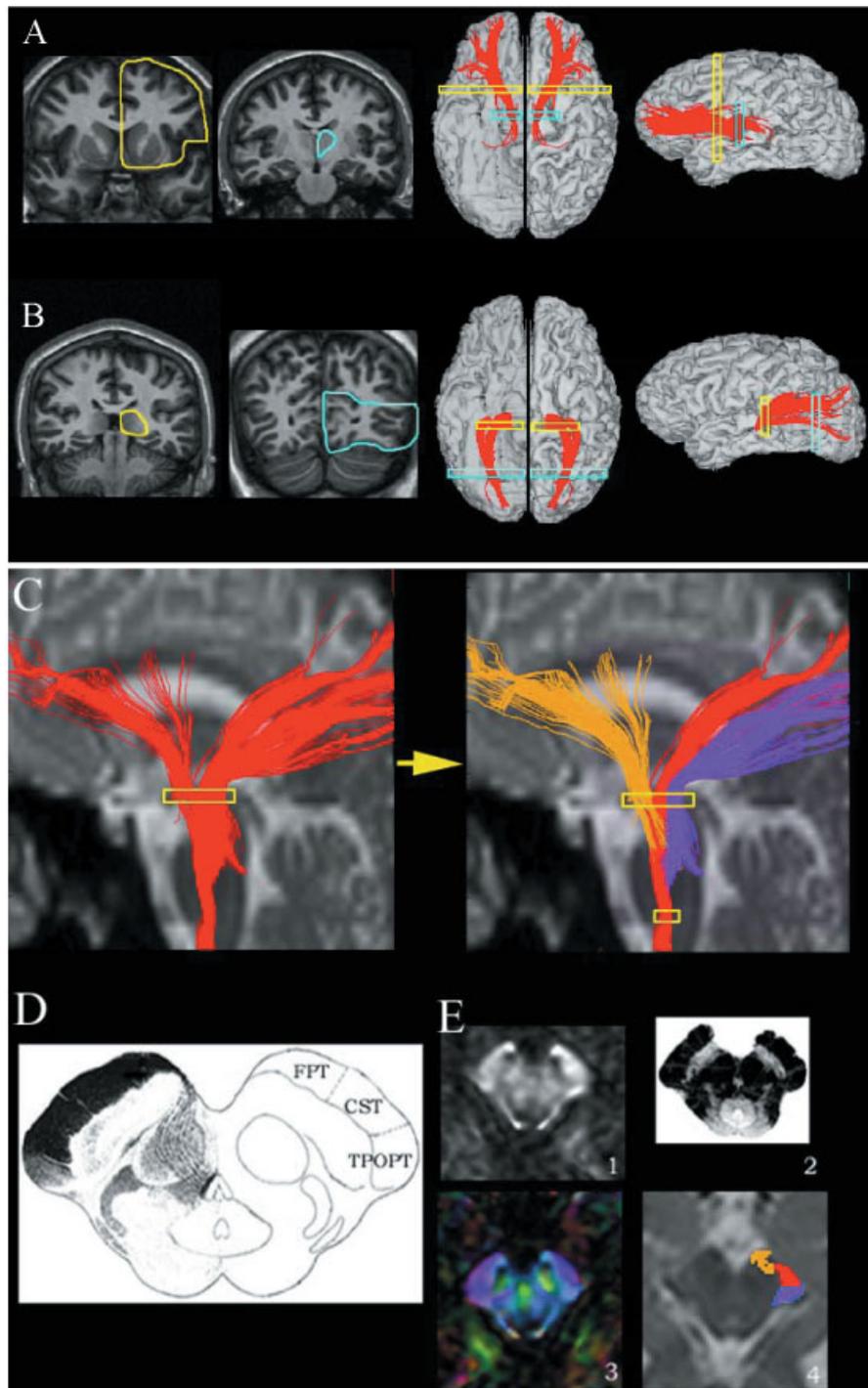
Figure 4. Example of using the multi-ROI approach to reconstruct white matter tracts of interest. Coronal images show the locations of two reference ROIs for each tract. The reconstruction results for the anterior (A) and posterior (B) thalamic radiation are presented in the axial and sagital view. Images in (C)–(E) show examples of the parcellation of homogeneous-looking white matter based on 3D tract trajectories. Results of tract reconstruction that penetrate the cerebral peduncle are shown in (C). Tracts excluded by the second ROI at the lower pons level are shown by green and blue. Yellow boxes indicate the locations of ROIs. The postulated parcellation of the cerebral peduncle based on anatomical studies is shown in (D). Images in (E) shows anisotropy map (E-1), histological preparation (E-2), color-coded map (E-3), and T_2-weighted image with the location of reconstructed results superimposed (E-4). The figures were reproduced from Mori et al.[52] (A,B), Stieltjes et al.[42] (C,E) and Carpenter[49] (D) with permission

gross anatomical knowledge of the tract trajectory is required. It also does not allow the elucidation of branching patterns in between the multiple ROIs.

By extending this approach, the technique sometimes allows one to distinguish multiple tracts that are running parallel at one point but have different destinations.[42] An example is shown in Fig. 4(C–E), where the cerebral peduncle is parcellated *in vivo* using tract tracing. It has been long postulated from anatomical studies that the cerebral peduncle should consist of three classes of axonal tracts. These are the corticospinal tract (CST) and projections from the pons to the frontal lobe (frontopontine tract, FPT), and from the pons to the parieto-, occipito- and temporal lobes (TPOPT), as shown in Fig. 4(D). If an initial ROI is placed on the entire cerebral peduncle, the reconstruction result contains all of these tracts. By using the information that only the CST reaches the lower pons and medulla, a second reference ROI can be placed in this region, which selects only the CST components from the initial result [Fig. 4(C)]. The resulting parcellation of the cerebral peduncle agrees very well with the postulated anatomy, as shown in Fig. 4(E). It should be stressed that such parcellation cannot be achieved using classical DTI, because the fibers run parallel and are not contrasted on anisotropy maps and color-coded maps. This parcellation by DTI can therefore only be done by the tracking technique, which can incorporate information distal to the ROI.

Energy minimization techniques

Fast marching technique.[37] Assume that ink is dropped on a cloth and a vector field can be visualized that indicates which way the ink is spreading. The speed for the spreading front propagation is defined by;

$$F(r) = A|\varepsilon_1(r) \cdot n(r)|$$

where A is the anisotropy, ε_1 is the eigenvector and n the orientation normal to the front.[37] This equation reflects that the spreading speed is largest when the propagating front line is co-linear with the eigenvector and minimal when it is perpendicular. Using this equation, the shape of the stain can be calculated from the vector field, which is equivalent to a contour line showing the distance from the origin traveled by the ink within the same amount of time. Multiple contour lines can be calculated, each representing the stain shape at a different time point. These multiple contours represent a likelihood-of-connection map. The most likely path between an arbitrary point to the seed pixel (origin of the stain) can be found by following the gradient of steepest path, similar to water flowing to a sink hole from arbitrary point in the sink.

Simulated annealing approach.[56] If two arbitrary points are chosen in a 2D vector field, what is the most favorable way to connect the two points? Although the simplest way is via a linear line, such a solution is most likely energetically unfavorable, because this line is probably not aligned with the true vector field. If the connection is allowed to be extremely flexible, there might be numerous lines that can connect the points with minimal energy. A path generated by this technique is based on the balance between the stiffness of the line and the energy minimization process (the more the line aligns to the vector field, the lower the energy). With an appropriate amount of allowed stiffness, the path should be able to find a way that can reproduce the correct tract trajectories. The best pathway is searched using simulated annealing, a technique that can minimize the effect of noise in a global fashion. Two initial POIs or ROIs are selected based on anatomical knowledge. Alternatively, the amount of the lowest energy can be used to estimate the 'likeliness' of the connection. For example, if two selected POIs are not connected by the real tract, the energy to force a connection between them must be large even for the energy minimized path. This approach can be extended to create a 'connectivity map'. More details of this approach have been given by Wedeen.[57]

LIMITATIONS AND SOLUTIONS

The techniques discussed in the previous chapter are all based on the principle that a clear principal axis can be defined inside an MRI voxel, that this voxel occupies a single tissue, and that the vector can be connected to a neighboring voxel. In practice, voxels are more likely to consist of contributions from multiple tissues (different white matter tracts, some CSF and gray matter, etc.) and signal-to-noise may be limited. In addition, there may not be a single predominant direction of water diffusion. In this chapter we deal with these issues and review some of the solutions and approaches that were recently suggested to address them.

Deviation from cigar-shape anisotropy[58]

The assumption that the direction of the largest principal axis aligns with a single local fiber orientation may not always be true. The most obvious case is when the data reveal two large eigenvalues and one small eigenvalue ($\lambda_1 = \lambda_2 > \lambda_3$) or, in other words, when a diffusion ellipsoid has a pancake shape rather than a cigar shape. In this case, the fiber orientation information about the largest and middle axes degenerates within a plane and the orientation of the largest principal axis is extremely sensitive to noise. As a consequence, it does not make sense to follow its orientation for the subsequent propagation. Until recently, this problem necessitated termination of tracking. To better quantify this judgment, indices for the cigar- (C_c) and planar- (C_p) shaped ellipsoids have been defined that allow the use of
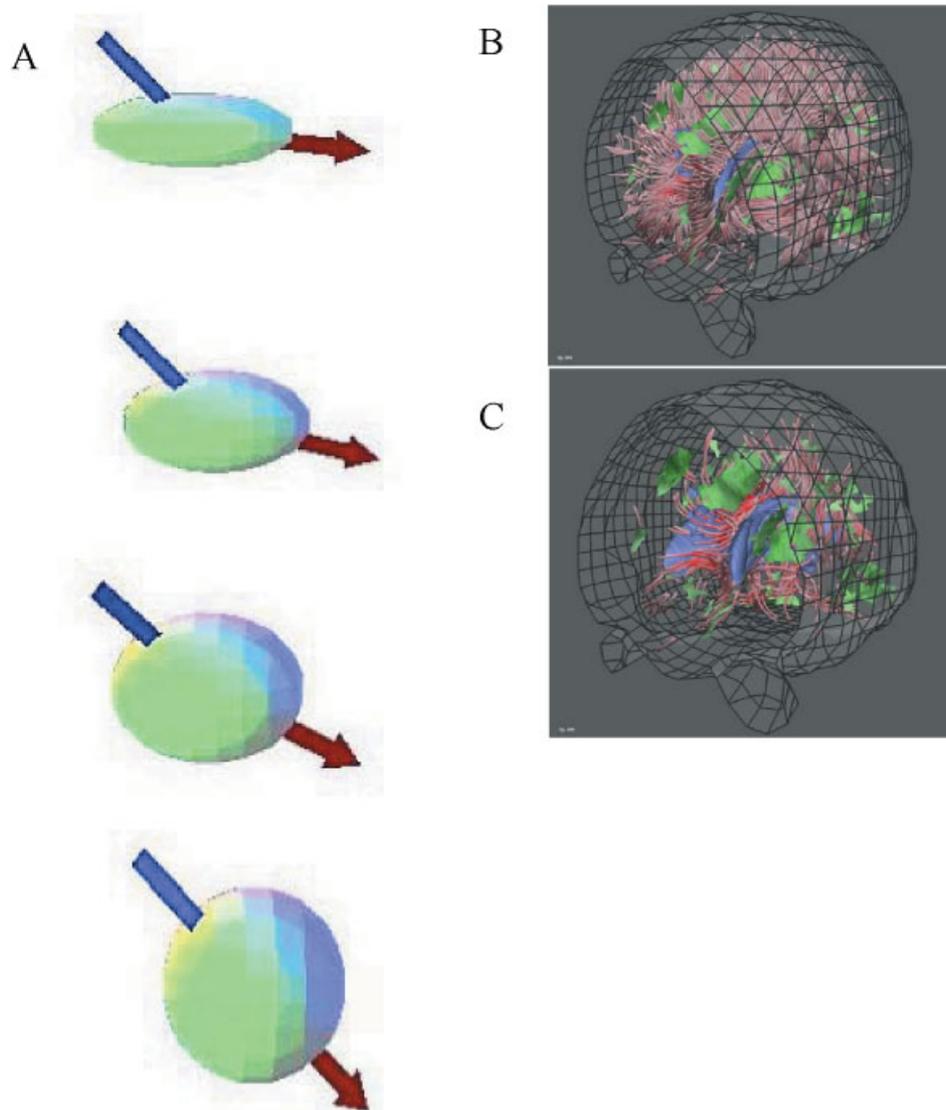
Figure 5. Examples of the behavior of the tensorline approach for different shapes of the diffusion ellipsoid (A). Incoming (v_{in}) and outgoing (v_{out}) vectors are indicated. Pictures were provided by courtesy of Dr Alexander, University of Wisconsin.[38] The image in (B) shows examples of streamtube (red) and streamsurface (green) visualization of the tensor field.[59] In (C), density of the streamtube was reduced to reveal internal structures. Ventricles are shown in blue for anatomical guidance. Images were provided courtesy of Dr Laidlow, Brown University

computer-based analysis of criteria such as $C_c <$ threshold, or $C_p >$ threshold:

$$C_c = \frac{\lambda_1 - \lambda_2}{\lambda_1 + \lambda_2 + \lambda_3}$$

$$C_p = \frac{2(\lambda_2 - \lambda_3)}{\lambda_1 + \lambda_2 + \lambda_3} \qquad (1)$$

For example, these parameters can be used as a threshold to prevent tracking in brain regions with low C_c or high C_p. Several new approaches to perform tracking in these areas with higher reproducibility have now been

postulated, which are discussed in the following paragraphs.

The tensor line technique.[38,58] In this approach, called 'tensorline', the incoming line orientation (v_{in}) is modulated according to the orientation of the diffusion ellipsoid, and the outgoing vector v_{out} is calculated according to the equation,

$$v_{out} = \overline{\overline{D}} v_{in} \qquad (2)$$

Figure 5(A) shows how this equation behaves in different situations. When $\overline{\overline{D}}$ is spherical or the incoming line is

parallel to the flat plane of the pancake-shaped ellipsoid, $v_{in} = v_{out}$. In other words, the line extrapolates the incoming direction, v_{in} and passes through the pixel without changing its orientation. If the incoming line hits the planar-shape ellipsoid from an oblique angle, it is deflected closer the plane of the flat surface of the ellipsoid. Recent studies have demonstrated that this approach can successfully reconstruct major fiber bundles and the results are more robust and reproducible under conditions of high noise.[38,53]

The surface line technique.[59] Assuming that the pancake shape of diffusion anisotropy is caused by a sheet-like structure of fibers, it may make more sense to propagate a sheet rather than a line. Such an approach, called streamsurfaces, was recently suggested by Laidlaw et al.,[59] who connected the diffusion ellipsoids with the pancake structure if neighboring pixels had the same characteristic shapes. The results could successfully locate and visualize white matter architectures with the cigar- and planar-type diffusion separately. Figure 5(B) and 5(C) shows examples of this approach.

The diffusion spectrum technique.[41,60] One possibility leading to coincidental occurrence of a pancake shape for the diffusion ellipsoid is the presence of a mixture of two or more populations of axonal tracts with different orientations. If there are more than three populations, the diffusion may seem even isotropic. Conventional DTI data acquisition and processing techniques cannot resolve such systems into the individual tract components. One technique to obtain more information on such a multi-component system was postulated by Wedeen et al.[41,61] In this so-called diffusion spectrum approach, signal intensity decay due to diffusion weighting is measured along more than 100 axes evenly spaced in the 3D space to directly define the extent of water diffusion along each axis. Similarly, it was demonstrated by Frank[60] that the degree of anisotropy can be directly estimated from the high angular resolution acquisition (43 orientations) without using tensor calculation. In this analysis, the deviations of the apparent diffusion constants along multiple orientations with respect to the average diffusion constant were used as an index of anisotropy. This quantity is called the spherical diffusion variance, $V = \langle D_{app}^2 \rangle - \langle D_{app} \rangle^2$, in which D_{app} is the apparent diffusion constant along multiple orientations that are equally distributed in 3D space. In the future, the direct determination of water diffusion properties in 3D space by the high angular resolution acquisition may provide a way to perform non-tensor-based fiber reconstruction, in which the tracking follows the orientation of the maximum diffusivity.

Other approaches to circumvent limitations imposed by multiple tract populations. When there are multiple populations of tracts within a pixel, the techniques discussed above can improve tractography results by detecting and visualizing such pixels (stream-surface technique), providing more robust tracking (tensorline technique), and better describing tract architecture within a pixel through an increased number of measurements (diffusion spectrum technique). However, as demonstrated by Basser et al.[35] simple unconstrained DTI tract tracing cannot distinguish whether two tracts are crossing or kissing within a pixel. In this situation, there are three options for researchers to choose. First, the tracking can be terminated when it hits a pixel with non-cigar-shape anisotropy. Second, anatomical knowledge can be used so that the tracking can penetrate the ambiguous pixels and connect pixels anterior and posterior to the ambiguous regions by finding a path with minimum energy.[34,56] Third, one should take into consideration the existence of consistent artifacts in the tracking results that go through particular anatomical regions. These artifacts may include missing branches and/or systematic mislabeling of adjacent tracts.

Erroneous results due to noise and resolution limitations

Assuming that there is no error in the DTI measurement process, there are still two major factors that may complicate the tractography. One is noise, and the other is the effect of partial voluming between different tissue types or fiber types. These errors are likely to be more significant for smaller tracts or for tracts close to the target gray matter (such as sub-cortical white matter), where white matter tracts tends to be more dispersed and narrower, with concomitant smaller anisotropies. Due to these problems, tracking results may deviate from the real tract trajectories.

Earlier, several tract reconstruction techniques were introduced, ranging from the simple linear line propagation model to the more sophisticated energy minimization approaches. The effect of noise is largest for the linear line propagation models and smaller for other techniques that use fitting, regularization and/or energy minimization processes. Partial volume effects (PVE) are directly related to the noise situation because image resolution must be increased to reduce PVE, leading to lower SNR. Post-processing enhancement of SNR will result in the reduction of resolution and, hence, increase PVE. Therefore, no matter which tracking technique is employed, the 3D reconstruction results are likely to always contain some data errors. In order to minimize these, the following two approaches have been proposed.

Knowledge-based multiple-ROI approach. Above, an editing technique based on multiple reference ROIs was explained. This approach imposes a significant constraint in the tract reconstruction, thereby effectively reducing the likelihood of the occurrence of erroneous
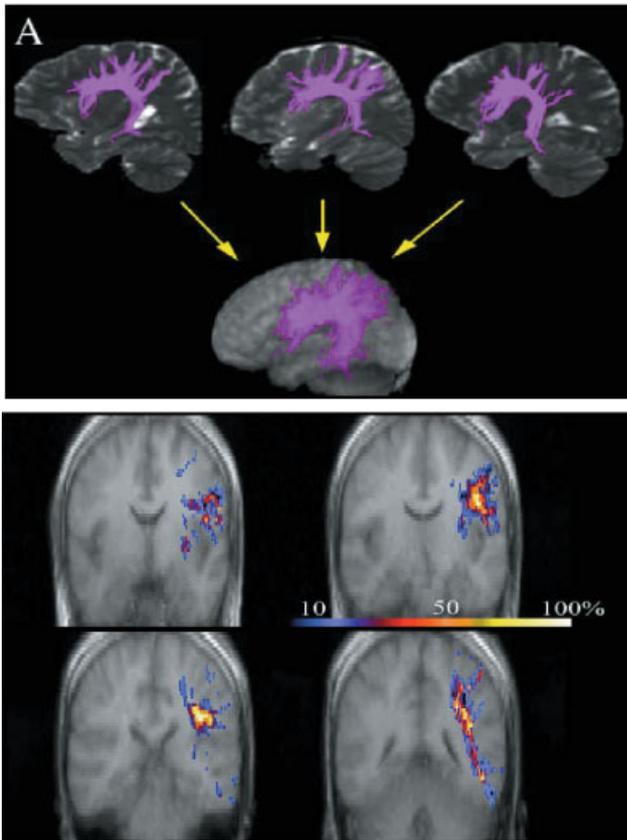
Figure 6. Application of the probabilistic approach to the superior longitudinal fascicules (SLF) of 10 normal volunteers. The reconstruction result from each individual was standardized into Talairach coordinates (A, B). The reconstructed SLF (A) and the probability of occurrence over 10 volunteers (B) are shown. It can be seen that some small branches have the lowest probability of 10%, indicating that these pixels had the SLF only 1 in the 10 subjects. Other branches, such as those in Broca's area and the temporal lobe, have high reproducibility (>50%). The figure was reproduced from Mori et al.[52] with permission

results. For example, if only one instead of two ROIs were to be used, the result could be more likely to contain not only the tract of interest but also many other tracts. Some may be erroneous due to noise and/or PVE, and some may be real trajectories of tracts that share the same ROI. These unwanted contributions can be effectively reduced by placing a second, or even third, reference ROI if the general trajectory of the tract of interest is known. The reason for using knowledge-based approaches is that once the tracking deviates from the real trajectory due to noise or PVE, it is highly unlikely that the real trajectory can be returned to by chance. A drawback of this approach is that it can, in many cases, be applied only to anatomically well-documented tracts, imposing limitations on the discovery of new tracts. However, the approach has a significant advantage in that the location of many tracts can be identified in living humans non-invasively.[32,39,42,52] In addition, in some cases even tracts that have large deviations, e.g. due to

the presence of tissue deformations, can still be reconstructed, as was recently demonstrated for a patient in which the cortical spinal tract was displaced by a meningeoma in the brain stem[42] and for patients with anaplastic astrocytomas.[61]

Probabilistic approach.[52] Assuming that errors due to noise and PVE are random, they are expected to have low reproducibility if the same subject is repeatedly scanned and the results are superimposed. If the shapes of individual brains can be normalized into one standard brain coordinate, they can be superimposed on each other to study the probability of having a tract of interest for each standard coordinate. An example of such an approach is shown in Fig. 6 where the superior longitudinal fasciculi of 10 healthy volunteers are reconstructed in Talairach coordinates. The data show excellent reproducibility for the large central bundles (probability as high as 100%), while smaller structures are often different between volunteers. While this is a promising approach to quantify and compare tracking results between populations, it should be noted that it is based on two techniques that are still under active development, namely the tract reconstruction itself and the brain normalization technique. Poor brain normalization quality may lead to obscure definition of smaller tracts of interest and, thus, lowering the power to detect abnormalities. These limitations become especially apparent for the smaller fiber structures near the cortical areas of the brain. Further improvements in both technical areas are therefore much needed.

THE ISSUE OF VALIDATION

There is no doubt that validation is of central importance for the development of tractography. For this purpose, we first have to evaluate what tractography provides us with and what the gold standard is to validate the results. As explained earlier, tractography can provide macroscopic neuroanatomical information of white matter structure. Specifically, it can parcellate the white matter into fiber structures that contain bundles of axonal tracts that are running largely in the same orientation. Given the current resolution of DTI, on the order of 1–5 mm per dimension, it is presently not possible to resolve white matter tracts into individual axons whose diameter is typically less than 10 μm.

There is accumulated knowledge about white matter anatomy based on slice-by-slice examination using histology.[48–50] Using a proper preparation, the tract structure can be appreciated and, for some fibers, the trajectory can be visually followed over many slices. More direct information about axonal connectivity can be obtained from animal lesion studies, in which degenerating axons with specific stains are visualized after placing lesions. The most elaborated information is obtained

using tract-tracing methods based on chemical tracers, in which chemicals such as radioactively labeled amino acids are injected and their destinations confirmed histologically. Obviously, these tract-tracing techniques cannot be applied to humans, where, most information has come from postmortem data on stroke patients. For connectivity studies, the chemical tracer techniques are considered one of the gold standards. Although it is in

principle possible to compare the results of this technique with the DTI-based tractography in animal models, there are several difficulties in such a validation approach. First, the chemical tracer techniques reveal connectivity at the cellular level. The axon of interest may merge into a white matter tract and again leave it from some points. The result of chemical tracing therefore represents only a tiny portion of axons in a white matter tract and, thus, it would not be surprising if the two results would not match. Second, the real advantage of the DTI-based tractography is its ability to quickly characterize the macroscopic white matter structures. It is virtually impossible to generate similar datasets (there are 10^{11} neurons inside a brain) using the single-cell level chemical tracer techniques. Considering these factors, one possible way to validate the results is to observe only the core of major white matter tracts using the tractography and compare them with anatomical knowledge, because trajectories and locations of the body of these tracts are fairly well known. Once the tracking data leaves the core and approaches the target gray matter regions, we do not have information to validate the results, especially for humans. Therefore, great care has to be taken. The statistical approach introduced earlier may prove to be a good technique to validate the results in terms of reproducibility.

Qualitative validation has been reported in animals[30,31] and humans,[32–34,37,38,40,42,56] and the results are very encouraging. One brain structure that is particularly suitable for the validation of the white matter tracts as measured by DTI is the brainstem, because of the simpler architecture and less complicated branching compared to the cerebral hemisphere. In Fig. 7, the 3D reconstruction results for five major white matter tracts in this brain structure are shown.[42] For these reconstructions, the techniques introduced earlier were used, namely tracts of interest were identified on DTI-based color maps and two reference ROIs were specified [Fig. 7(C)] based on the
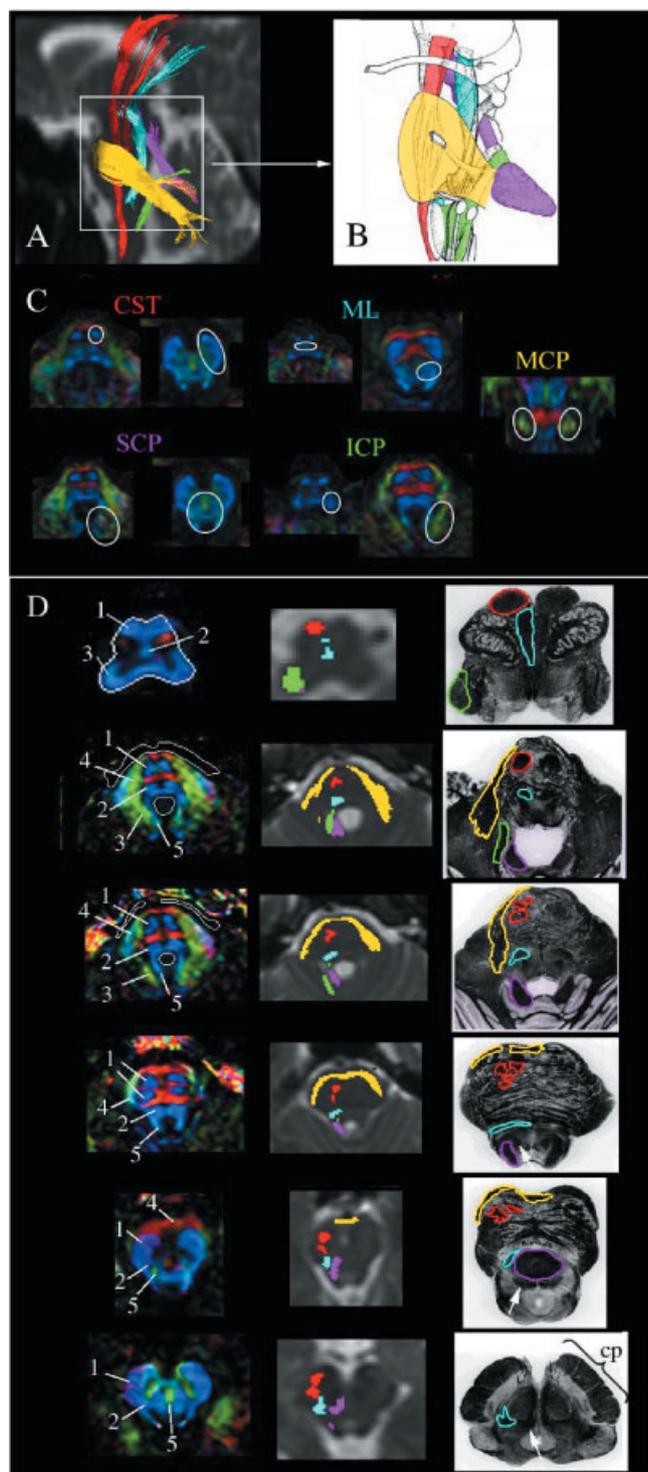

Figure 7. Three-dimensional reconstruction of five major tracts in the brainstem (A) and comparison with anatomy (B). Locations of ROIs used for each tract are shown in (C). Color coding and abbreviations are: red, corticospinal tract (CST); blue, medial lemniscus (ML); pink, superior cerebellar peduncle (SCP); yellow, middle cerebellar peduncle (MCP); and green, inferior cerebellar peduncle (ICP). In the color maps in (C), blue represents tracts orienting the rostral–caudal direction, red right–left, and green ventral–dorsal. Images in (D) show comparison between the DTI-based tract reconstruction and anatomical preparation at five representative slices. The first column shows color maps: 1, corticospinal tract; 2, medial lemniscus; 3, inferior cerebellar peduncle; 4, middle cerebellar peduncle; and 5, superior cerebellar peduncle. The second column shows locations of reconstructed tracts superimposed on T_2-weighted images. The third column shows anatomical preparations,[64] in which locations of the tracts of interest are indicated by the color coding. (B) and anatomical preparation in (D) are reproduced from Nieuwenhuys et al.[51] and Williams et al.[64] with permission

known trajectories of these tracts [Fig. 7(B)]. Subsequently, an exhaustive search was performed to identify all tracts that penetrate the two ROIs. The results of this approach [Fig. 7(A)] agree well with the known histology-based anatomy of these tracts [Fig. 7(C)]. The slice-by-slice comparison between the tractography and anatomical preparation shown in Fig. 7(D) further supports the validity of the DTI approach.

Comparison studies between a manganese-based tracking technique and DTI was also reported recently.[62] The study showed that the DTI could correctly determine the fiber orientation with less than 10% of deviation for a SNR of 40 or greater. Probably the ideal validation study may require a phantom, in which such uncertainties as the effect of motions and partial volume effect structures can be removed, although such a phantom is currently not available.

SUMMARY AND CONCLUSIONS

In this chapter, several DTI tractography techniques were discussed that are presently being used for white matter tract tracing. As the field of tract tracing by DTI is rather young, it is expected that many new technologies will be developed in the near future. However, recent results have shown that even the simple methodologies reviewed here are already able to visualize major white matter connections *in situ* in animals and humans. For instance, the brainstem fibers and several of the cortico-cortical association fibers have recently been reported, including the corpus callosum, thalamic radiations, corticospinal tracts, association fibers, and cerebellar peduncles.[31–42,55] Upon using these exciting data to investigate specific neuroanatomical questions, it is very important to keep in mind the limitations of the DTI method used to acquire them. First of all, this technique can be used only for macroscopic analysis of white matter architecture, but not to address connectivity questions at the cellular level. One particularly limiting problem related to this macroscopic character of DTI is the mixing of axonal tracts with different orientations within a pixel. DTI may be able to locate where these problematic pixels are, but it is difficult to decipher axonal information in such pixels. On the other hand, there are some approaches that circumvent this issue under favorable conditions, such as the use of reference ROI placement based on prior knowledge. The most important conclusion that can be drawn in this initial phase of the field is that DTI tractography can indeed delineate the core of large white matter tracts as judged from the encouraging results from initial validation studies. At present, there are no other non-invasive techniques that can provide equivalent information and, as a consequence, DTI tractography is expected to be a powerful technique to investigate white matter anatomy and disease in situ in humans.

REFERENCES

1. Tanner JE. Self diffusion of water in frog muscle. *Biophys. J.* 1979; **28**: 107–116.
2. Scollan DF, Holmes A, Winslow R, Forder J. Histological validation of myocardial microstructure obtained from diffusion tensor magnetic resonance imaging. *Am. J. Physiol.* 1998; **275**: H2308–2318.
3. Moseley ME, Cohen Y, Kucharczyk J, Mintorovitch J, Asgari HS, Wendland MF, Tsuruda J, Norman D. Diffusion-weighted MR imaging of anisotropic water diffusion in cat central nervous system. *Radiology* 1990; **176**: 439–445.
4. Basser PJ, Mattiello J, LeBihan D. Estimation of the effective self-diffusion tensor from the NMR spin echo. *J. Magn. Reson. B* 1994; **103**: 247–254.
5. Basser PJ, Mattiello J, Le Bihan D. MR diffusion tensor spectroscopy and imaging. *Biophys. J.* 1994; **66**: 259–267.
6. van Gelderen P, de Vleeschouwer MH, DesPres D, Pekar J, van Zijl PCM, Moonen CTW. Water diffusion and acute stroke. *Magn. Reson. Med.* 1994; **31**: 154–163.
7. van Zijl PCM, Davis D, Moonen CTW. *NMR in Physiology and Biomedicine*, Gillies RJ (ed.). Academic Press: San Diego, CA, 1994; 185–198.
8. Mori S, van Zijl PCM. Diffusion weighting by the trace of the diffusion tensor within a single scan. *Magn. Reson. Med.* 1995; **33**: 41–52.
9. Neil J, Shiran S, McKinstry R, Schefft G, Synder A, Almli C, Akbudak E, Arnovitz J, Miller J, Lee B, Conturo T. Normal brain in human newborns: apparent diffusion coefficient and diffusion anisotropy measured by using diffusion tensor MR imaging. *Radiology* 1998; **209**: 57–66.
10. Neil JM, Mukherjee P, Huppi PS. Diffusion tensor imaging of normal and injured developing human brain. *NMR Biomed.* 2002; **15**: 543–552.
11. Clark C, Werring D, Miller D. Diffusion imaging of the spinal cord in vivo: estimation of the principal diffusion and application to multiple sclerosis. *Magn. Reson. Med.* 2000; **43**: 133–138.
12. Tievsky A, Ptak T, Farkas J. Investigation of apparent diffusion coefficient and diffusion tensor anisotrophy in acute and chronic multiple sclerosis lesions. *Am. J. Neuroradiol.* 1999; **20**: 1491–1499.
13. Ellis C, Simmons A, Jones D, Bland J, Dawson J, Horsfield M, Williams S, Leigh P. Diffusion tensor MRI assesses corticospinal tract damages in ALS. *Neurology* 1999; **22**: 1051–1058.
14. Mukherjee P, Bahn MM, McKinstry RC, Shimony JS, Cull TS, Akudak E, Snyder AZ, Conturo TE. Difference between gray matter and white matter water diffusion in stroke: diffusion tensor MR imaing in 12 patients. *Radiology* 2000; **215**: 211–220.
15. Sotak CH. The role of diffusion tensor imaging in the evaluation of ischemic brain injury. *NMR Biomed.* 2002; **15**: 561–569.
16. Lim KO, Hedehus M, Moseley M, de Crespigny A, Sullivan EV, Pfefferbaum A. Compromised white matter tract integrity in schizophrenia inferred from diffusion tensor imaging. *Arch. Gen. Psychiat.* 1999; **56**: 367–374.
17. Horsfield MA, Jones DK. Applications of diffusion-weighed and diffusion tensor MRI to white matter diseases. *NMR Biomed.* 2002; **15**: 570–577.
18. Klingberg T, Hedehus M, Temple E, Salz T, Gabrieli J, Moseley M, Poldrack R. Microstructure of temporo-parietal white matter as a basis for reading ability: evidence from diffusion tensor magnetic resonance imaging. *Neuron* 2000; **25**: 493–500.
19. Ulug AM, Beauchamp N Jr., Bryan RN, van Zijl PC. Absolute quantitation of diffusion constants in human stroke. *Stroke* 1997; **28**: 483–90.
20. Baird AE, Warach S. Magnetic resonance imaging of acute stroke. *J. Cereb. Blood Flow Metab.* 1998; **18**: 583–609.
21. Albers GW, Lansberg MG, Norbash AM, Tong DC, O'Brien MW, Woolfenden AR, Marks MP, Moseley ME. Yield of diffusion-weighted MRI for detection of potentially relevant findings in stroke patients. *Neurology* 2000; **54**: 1562–1567.
22. Wu O, Koroshetz WJ, Ostergaard L, Buonanno FS, Copen WA, Gonzalez RG, Rordorf G, Rosen BR, Schwamm LH, Weisskoff RM, Sorensen AG. Predicting tissue outcome in acute human cerebral ischemia using combined diffusion- and perfusion-weighted MR imaging. *Stroke* 2001; **32**: 933–42.

23. Pierpaoli C, Basser PJ. Toward a quantitative assessment of diffusion anisotropy. *Magn. Reson. Med.* 1996; **36**: 893–906.

24. Ulug A, van Zijl PCM. Orientation-independent diffusion imaging without tensor diagonalization: anisotropy definitions based on physical attributes of the diffusion ellipsoid. *J. Magn. Reson. Imag.* 1999; **9**: 804–813.

25. Douek P, TR, Pekar J, Patronas N, Le Bihan D. MR color mapping of myelin fiber orientation. *J. Comput. Assist. Tomogr.* 1991; **15**: 923–929.

26. Nakada T, Matsuzawa H. Three-dimensional anisotropy contrast magnetic resonance imaging of the rat nervous system: MR axonography. *Neurosci. Res.* 1995; **22**: 389–398.

27. Pajevic S, Pierpaoli C. Color schemes to represent the orientation of anisotropic tissues from diffusion tensor data: application to white matter fiber tract mapping in the human brain. *Magn. Reson. Med.* 1999; **42**: 526–540.

28. Mori S, Crain BJ, van Zijl PC. 3D brain fiber reconstruction from diffusion MRI. In *Proceedings of International Conference on Functional Mapping of the Human Brain*, Montreal, 1998.

29. Basser JB. Fiber-tractography via diffusion tensor MRI. In *Proceedings of International Society for Magnetic Resonance in Medicine*, Sydney, 1998; 1226.

30. Mori S, Crain BJ, Chacko VP, van Zijl PCM. Three dimensional tracking of axonal projections in the brain by magnetic resonance imaging. *Ann. Neurol.* 1999; **45**: 265–269.

31. Xue R, van Zijl PCM, Crain BJ, Solaiyappan M, Mori S. *In vivo* three-dimensional reconstruction of rat brain axonal projections by diffusion tensor imaging. *Magn. Reson. Med.* 1999; **42**: 1123–1127.

32. Conturo TE, Lori NF, Cull TS, Akbudak E, Snyder AZ, Shimony JS, McKinstry RC, Burton H, Raichle ME. Tracking neuronal fiber pathways in the living human brain. *Proc. Natl Acad. Sci. USA* 1999; **96**: 10422–10427.

33. Mori S, Kaufmann WK, Pearlson GD, Crain BJ, Stieltjes B, Solaiyappan M, van Zijl PCM. *In vivo* visualization of human neural pathways by MRI. *Ann. Neurol.* 2000; **47**: 412–414.

34. Poupon C, Clark CA, Frouin V, Regis J, Bloch L, Le Bihan D, Mangin JF. Regularization of diffusion-based direction maps for the tracking of brain white matter fascicules. *NeuroImage* 2000; **12**: 184–195.

35. Basser PJ, Pajevic S, Pierpaoli C, Duda J, Aldroubi A. In vitro fiber tractography using DT-MRI data. *Magn. Reson. Med.* 2000; **44**: 625–632.

36. Jones DK, Simmons A, Williams SC, Horsfield MA. Non-invasive assessment of axonal fiber connectivity in the human brain via diffusion tensor MRI. *Magn. Reson. Med.* 1999; **42**: 37–41.

37. Parker GJ. Tracing fiber tracts using fast marching. In *Proceedings, International Society of Magnetic Resocance*, Denver, CO, 2000; 85.

38. Lazar M, Weinstein D, Hasan K, Alexander AL. Axon tractography with tensorlines. In *Proceedings of International Society of Magnetic Resonance in Medicine*, Denver, CO, 2000; 482.

39. Werring DJ, Toosy AT, Clark CA, Parker GJ, Barker GJ, Miller DH, Thompson AJ. Diffusion tensor imaging can detect and quantify corticospinal tract degeneration after stroke. *J. Neurol. Neurosurg. Psychiat.* 2000; **69**: 269–272.

40. Tuch DS, Belliveau JW, Wedeen V. A path integral approach to white matter tractography. In *Proceedings of International Society of Magnetic Resonance in Medicine*, Denver, CO, 2000; 791.

41. Wedeen V, Reese TG, Tuch DS, Weigel MR, Dou JG, Weiskoff RM, Chessler D. Mapping fiber orientation spectra in cerebral white matter with fourier-transform diffusion MRI. In *Proceedings of International Society of Magnetic Resonance in Medicine*, Denver, CO, 2000; p. 82.

42. Stieltjes B, Kaufmann WE, van Zijl PCM, Fredericksen K, Pearlson GD, Mori S. Diffusion tensor imaging and axonal tracking in the human brainstem. *NeuroImage* 2001; **14**: 723–735.

43. Beaulieu C. The basis of anisotropic water diffusion in the nervous system. *NMR Biomed.* 2002; **15**: 435–455.

44. Chenevert TL, Brunberg JA, Pipe JG. Anisotropic diffusion in human white matter: Demonstration with MR technique in vivo. *Radiology* 1990; **177**: 401–405.

45. Doran M, Hajnal JV, van Bruggen N, King MD, Young IR, Bydder GM. Normal and abnormal white matter tracts shown by MR imaging using directional diffusion weighted sequences. *J. Comput. Assist. Tomogr.* 1990; **14**: 865–873.

46. Pierpaoli C, Jezzard P, Basser PJ, Barnett A, Di Chiro G. Diffusion tensor MR imaging of human brain. *Radiology* 1996; **201**: 637–648.

47. Makris N, Worth AJ, Sorensen AG, Papadimitriou GM, Reese TG, Wedeen VJ, Davis TL, Stakes JW, Caviness VS, Kaplan E, Rosen BR, Pandya DN, Kennedy DN. Morphometry of in vivo human white matter association pathways with diffusion weighted magnetic resonance imaging. *Ann. Neurol.* 1997; **42**: 951–962.

48. Crosby E, Humphrey T, Lauer E. Correlative anatomy of the nervous system. Macmillan: New York, 1962.

49. Carpenter M. Human neuroanatomy. Baltimore, MD: Williams & Wilkins, 1976.

50. Nieuwenhuys R, Voogd J, van Huijzen C. The Human Central Nervous System. Springer: Berlin, 1983.

51. Lori NF, Akbuda E, Snyder AZ, Shimony JS, Conturo TE. Diffusion tensor tracking of human neuronal fiber bundles: Simulation of effects of noise, voxel size and data interpolation. In *Proceedings, International Society of Magnetic Resonance in Medicine*, Denver, CO, 1999; 775.

52. Mori S, Kaufmann WE, Davatzikos C, Stieltjes B, Amodei L, Fredericksen K, Pearlson GD, Melhem ER, Solaiyappan M, Raymond GV, Moser HW, van Zijl PCM. Imaging cortical association tracts in human brain. *Magn. Reson. Imag.* 2002; **47**: 215–223.

53. Lazar M, Alexander AL. Error analysis of white matter tracking algorithms (streamlines and tensorlines) for DT-MRI. In *Proceedings of International Society of Magnetic Resonance in Medicine, Glasgow, UK*, 2001; 506.

54. Mangin J-F, Poupon C, Riviere D, Ppadopoulos-Orfanos D, Clark CA, Regis J, Le Bihan D. Spin glass models for the inference of anatomical connectivities matrices from diffusion-weighted MR data. *NMR Biomed.* 2002; **15**: 481–492.

55. Holodny AI, Ollenschleger MD, Liu WC, Schulder M, Kalnin AJ. Identification of the corticospinal tracts achieved using blood-oxygen- level-dependent and diffusion functional MR imaging in patients with brain tumors. *Am. J. Neuroradiol.* 2001; **22**: 83–88.

56. Tuch DS, Wiegell MR, Reese TG, Belliveau JW, Wedeen V. Measuring cortico-cortical connectivity matrices with diffusion spectrum imaging. In *Proceedings of International Society of Magnetic Resonance in Medicine*, Glasgow, UK, 2001; 502.

57. Wedeen V. Imaging crossing fibers. *NMR Biomed.* (in press).

58. Weinstein D, Kindlmann G, Lundberg EC. Tensorlines: advection diffusion based propagation through diffusion tensor fields. In *Proceedings, IEEE Visualization*, San Francisco, CA, 1999; p. 249–253.

59. Zhang S, Laidlaw D. Elucidating neural structure in diffusion tensor MRI volumes using streamtubes and streamsurfaces. In *Proceedings of International Society of Magnetic Resonance in Imaging*, Glasgow, UK, 2001; 505.

60. Frank LR. Anisotropy in high angular resolution diffusion-weighted MRI. *Magn. Reson. Med.* 2001; **45**: 935–939.

61. Mori S, Fredericksen K, van Zijl PC, Stieltjes B, kraut AK, Solaiyappan M, Pomper MD. Brain white matter anatomy of tumor patients using diffusion tensor imaging. *Ann. Neurol.* 2002; **51**: 377–380.

62. Lin CP, Tseng WY, Cheng HC, Chen JH. Validation of diffusion tensor magnetic resonance axonal fiber imaging with registered manganese-enhanced optic tracts. *Neuroimage* 2001; **14**: 1035–1047.

63. Albert B, Bray D, Lewis J, Raff M, Roberts K, Watson JD. Molecular Biology of the Cell. Garland Publishing: New York, 1989.

64. Williams TH, Gluhbegovic N, Jew JY. The human brain: dissections of the real brain. *Vitrual Hospital, University of Iowa*, 1997; www.vh.org/Providers/Textbooks/BrainAnatomy and www.brain-university.com [21/10/00]